Enzyme and Microbial Technology 66 (2014) 48–55

Contents lists available at ScienceDirect

Enzyme and Microbial Technology

journal homepage: www.elsevier.com/locate/emt

Zirconia-poly(propylene imine) dendrimer nanocomposite based electrochemical urea biosensor

Sudheesh K. Shukla, Ajay K. Mishra, Bhekie B. Mamba, Omotayo A. Arotiba*

Department of Applied Chemistry, Doornfontein Campus 2028, University of Johannesburg, Johannesburg, South Africa

ARTICLE INFO

Article history:
Received 9 March 2014
Received in revised form 13 August 2014
Accepted 14 August 2014
Available online 27 August 2014

Keywords:
Electrochemical biosensor
Urea
Urease enzyme
ZrO_2 nanoparticle
Poly (propylene imine) dendrimer
Nanocomposite
Electro-co-deposition

ABSTRACT

In this article we report a selective urea electrochemical biosensor based on electro-co-deposited zirconia-polypropylene imine dendrimer (ZrO_2-PPI) nanocomposite modified screen printed carbon electrode (SPCE). ZrO_2 nanoparticles, prepared by modified sol–gel method were dispersed in PPI solution, and electro-co-deposited by cyclic voltammetry onto a SPCE surface. The material and the modified electrodes were characterised using FTIR, electron microscopy and electrochemistry. The synergistic effect of the high active surface area of both materials, i.e. PPI and ZrO_2 nanoparticles, gave rise to a remarkable improvement in the electrocatalytic properties of the biosensor and aided the immobilisation of the urease enzyme. The biosensor has an ampereometric response time of ~4 s in urea concentration ranging from 0.01 mM to 2.99 mM with a correlation coefficient of 0.9985 and sensitivity of 3.89 $\mu A\,mM^{-1}\,cm^{-2}$. The biosensor was selective in the presence of interferences. Photochemical study of the immobilised enzyme revealed high stability and reactivity.

1. Introduction

The estimation of urea concentration in serum or urine is essential for the diagnosis of kidney and liver diseases [1,2]. Abnormally high urea levels (the normal range in the blood being 8 mg dL^{-1}–20 mg dL^{-1}) can cause the obstruction of the urinary tract, shock, burns, gastrointestinal bleeding, dehydration, and renal failure. On the other hand, a decrease in the level of urea can cause nephritic syndrome, cachexia, and hepatic failure. Since both high and low concentrations of urine pose health risks, the estimation of urea levels in the blood/serum/urine is therefore important for the assessment of kidney functions and the diagnosis of different kidney related diseases [3,4]. In addition to medical diagnoses, the estimation of urea is an important parameter in other fields such as the food industry, pharmaceuticals, as well as in environmental protection and monitoring.

Several conventional methods such as fluorometric and chromatographic analyses have been reported for urea detection in tissue and body fluids. These detection techniques can sometimes be complicated with extensive sample pre-treatment and may be unsuitable for on-line monitoring. In response to these challenges, electrochemical biosensors have gained increasing interest as an alternative to conventional detection methods due to their comparative low cost, high sensitivity and simplicity [5,6]. The performances of electrochemical biosensors however need to be improved for more real life and versatile applications. One of the approaches used in the optimisation of biosensors is the incorporation of nanomaterials especially as immobilisation layers where they are expected to increase surface area for better biomolecule (e.g. enzyme) adsorption and loading; and promote faster electron transfer between the electrode and the active site of the enzyme [7,8]. Various inorganic nanomaterials such as Au, Ag, Fe_3O_4, ZnO, ZrO_2 [7–12] and organic polymer nanostructures such as dendrimer [13–15] have been used in the development of electrochemical biosensors. Dendrimers [16,17] are an exciting new class of three dimensional, highly branched, nanoscale, globular shaped and macromolecular architecture that emanates from a central core, and has a definite number of generations and functional end groups. A typical example is poly(propylene imine) (PPI) which has a tertiary inner amine branch and a peripheral primary amine (Scheme 1).

Depending on the properties sought, a nanomaterial can be combined with other materials (which may or may not be in the nanoscale) to form nanocomposites which can greatly improve the immobilisation layer in a biosensor. For example, a polymer such as chitosan has been combined with ZrO_2 in a glucose biosensor as an inorganic–organic nanocomposite (ION) immobilisation matrix where the polymer was used to entrap the metal

* Corresponding author. Tel.: +27 11 559 6200; fax: +27 11 559 6425.
E-mail addresses: oarotiba@uj.ac.za, omotayoarotiba@gmail.com (O.A. Arotiba).

http://dx.doi.org/10.1016/j.enzmictec.2014.08.003
0141-0229/

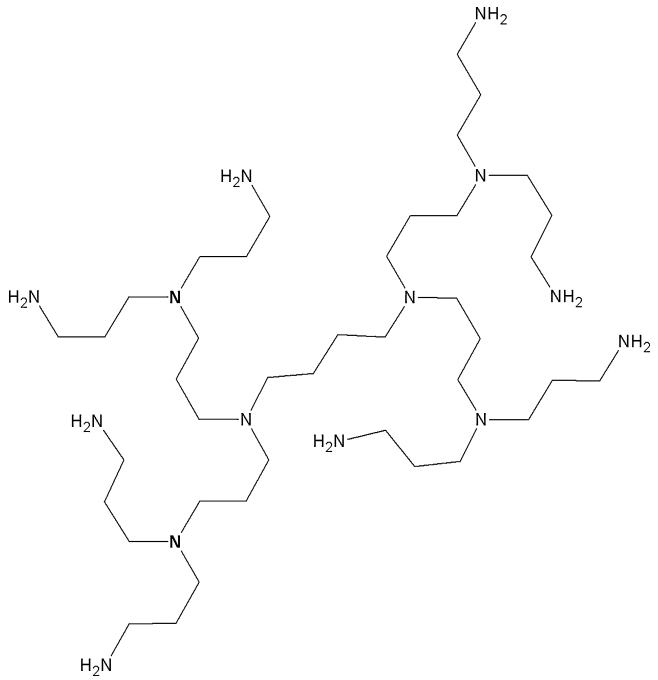

Scheme 1. Chemical structure of generation 1 Poly(propylene imine) dendrimer.

oxide nanoparticle [11]. Owing to their host–guest abilities, dendrimers are therefore nanomaterials of choice in the preparation of ION and such nanocomposites have been reported in literature either for biosensors [18] or other catalytic purposes [19]. In a dendrimer nanocomposite, the dendrimers can serve as the biocompatible layer, nano-encapsulator and covalent attachment site for the immobilisation of bioreceptors and modification of the electrode as well [20].

This article focuses on harnessing the properties of ZrO_2 nanoparticle and poly(propylene imine) dendrimers by preparing a novel inorganic-organic nanocomposite matrix based on ZrO_2/PPI for development of an electrochemical urease enzyme biosensor.

2. Materials and methods

2.1. Reagents and preparation of solutions

The following were purchased from Sigma–Aldrich (St. Louis, Montana, USA) and were used without further purification: urease (Aldrich, from *Canvalia ensiformis*), urea, Generation 2 (G2) poly(propylene imine) (PPI) dendrimer (SyMO-Chem, Eindhoven, Netherland), glutaraldehyde, uric acid, zirconium (IV) nitrate [$Zr(NO_3)_4{\cdot}3H_2O$], ethylene glycol, HNO_3, ammonia solution, potassium chloride, dipotassium hydrogen phosphate, potassium dihydrogen phosphate, potassium ferricyanide, potassium ferrocyanide. Phosphate buffer solution (PBS) (10 mM, pH 7.0) and ferri/ferro cyanide solution were used as supporting electrolytes for all amperometric measurements. Milli-Q water (18.2 MΩ/cm^2 at 25 °C) deionized water was used to prepare all the aqueous solutions. All the glassware and solutions were autoclaved prior to being used.

2.2. Instrumentation

The particle phase, size, and structure of synthesised ZrO_2 nanoparticles were studied using X-ray powder diffraction patterns on an X-ray diffractometer (Rigagu Ultima IV) with Cu Kα (λ = 1.5405 Å) radiation and transmission electron microscopy (TEM) (Jeol model, JEM-2100F) respectively. Fourier transform infrared (FTIR) spectra were obtained from PerkinElmer spectrum 100 spectrophotometer (PerkinElmer, Waltham, MA, USA). The IR spectra were recorded on an IR universal ATR sampling system accessory transmission mode with an accumulation of 16 scan and a resolution of 4 cm^{-1} in the range of 4000 cm^{-1} to 450 cm^{-1}.

The surface morphology of the electrode was examined by scanning electron microscopy (SEM) TESCAN (Vega 3 XMU) operated at 20 kV and the samples were sputter-coated with thin layer of carbon. Electrodeposition and all electrochemical measurements (CV, impedance, and amperometric measurements) were performed using an IVIUM CompactStat electrochemical workstation (Ivium Technologies B.V., Netherland). Screen printed electrodes (DRP-110) were purchased from DROPSENS. Platinum wire and Ag/AgCl (3 M KCl) were used as auxiliary and reference electrode respectively. Amperometric studies were performed under stirred conditions and all the solutions were purged with high purity argon gas for at least 15 min before electrochemical measurements were done.

2.3. Synthesis of ZrO_2 nanoparticles

ZrO_2 nanoparticles have been prepared by adopting a modified sol-gel methods. An analytical grade of $Zr(NO_3)_4{\cdot}3H_2O$ (0.98 mmol) was dissolved in 0.1 M HNO_3 (10 ml). A 1 mL volume of ethylene glycol was added and the mixture was stirred for 45 min. Then 25% ammonia solution was added to the mixture with continuous stirring by using magnetic stirrer at room temperature to adjust the pH to 8. The suspension was stirred at room temperature for 30 min and the resultant suspension was allowed to dry in an oven at 100 °C for 12 h and further annealed at 600 °C for 2 h.

2.4. Preparation of ZrO_2/PPI dendrimer solution

ZrO_2 nanoparticle was dispersed in 30 mM solution PPI in a mass to volume ratio of 1:100 where a typical mixture was 0.30 g ZrO_2 in 30 mL PPI. The mixture was stirred for one hour at room temperature after which it was sonicated for 20 min. Finally, a highly dispersed colloidal solution was formed.

2.5. Preparation of ZrO_2/PPI dendrimer modified SPE

Prior to the electrode modification, the bare SPCE was electrochemically cleaned by cyclic voltammetry using a potential range of −200 mV to +1500 mV in a solution of 0.5 H_2SO_4 for five consecutive cycles. The cleanliness of the surface was verified in the PBS (10 mM, pH 7.5) by using potential sweep in the range of −0.1 V to 0.65 V at a scan rate of 50 mV s^{-1} where no peak was expected. Finally, the electrode was thoroughly washed with deionized water and dried in an oven at 50 °C for five minutes. ZrO_2/PPI hybrid nanocomposites modified SPCE were then fabricated by using electro-co-electrodeposition methods according to the modified procedure reported by Arotiba et al. [20,21] in the following manner: 50 μL of a viscous mixture of ZrO_2 nanoparticles and 30 mM PPI dendrimer (molar ratio 1:100) was pipetted onto the pre-cleaned SPCE. This was followed by cyclic voltammetry (CV) between potential sweeps −0.3 V to 1.500 V for 20 cycles at a 50 mV s^{-1} scan rate. The preparation of the ZrO_2-PPI dendrimer/SPCE system involved the simultaneous electro-co-deposition of PPI and ZrO_2 on a clean SPCE. These ZrO_2/PPI modified SPCE was rinsed repeatedly with de-ionized water and PBS respectively, to remove the physically unbound (or any weakly bound) particles. A freshly prepared electrode was used in all the respective electrochemical studies.

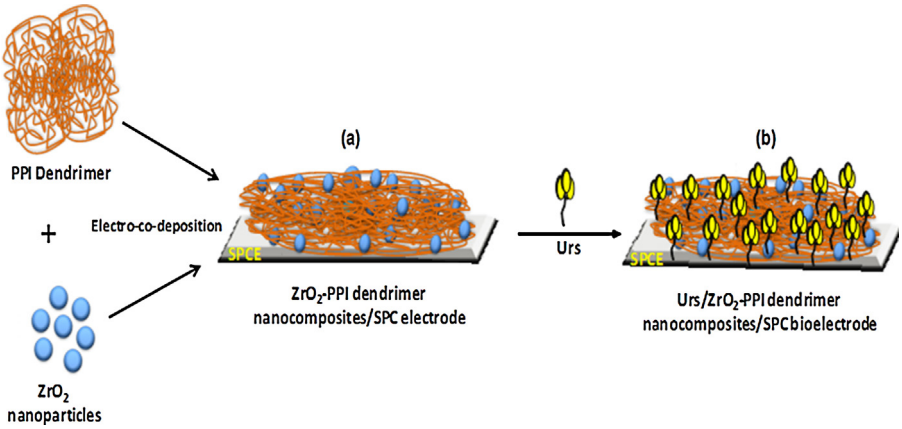

Scheme 2. Schematic illustration of (a) fabrication of ZrO_2-PPI dendrimer/SPC electrode, and (b) immobilization of Urease on ZrO_2-PPI dendrimer nanocomposite electrode.

2.6. Immobilisation of Urease onto ZrO_2/PPI dendrimer SPC bio-active electrode

The urea bioactive electrode was prepared by covalent immobilisation of the urease enzyme with the ZrO_2-PPI electrode surface using glutaraldehyde as a linker. 10 μL of 25% glutaraldehyde solution was spread over the ZrO_2-PPI modified SPCE and kept for five hours at room temperature. This was followed by dropping 20 μL of freshly prepared urease enzyme (10 mg mL^{-1} in Tris buffer [5 mM]) spread on the surface of the ZrO_2-PPI/SPCE. The Urease/ZrO_2-PPI/SPC (i.e. biosensor) was kept undisturbed and left to dry at 4 °C for about 15 hrs. Finally, this urea biosensor was washed by PBS (50 mM, pH 7.0) in order to remove any unbound enzymes from the biosensor electrode surface. Scheme 2 is focused on the preparation of ZrO_2-PPI nanocomposite for the immobilisation of urease onto ZrO_2-PPI nanocomposite.

2.7. Spectrophotometric Response studies

For photometric measurements, the biosensor (Urease/ZrO_2-PPI/SPCE) was dipped in a 5 mL phosphate buffer solution (50 mM, pH 7.0) containing 250 μL Nessler's reagent and 1 mL of urea solution (with varying concentrations). After 3 min of incubation, the absorbance of the coloured product ($NH_2Hg_2I_3$, a complex formed between the Nessler's reagent and ammonia produced after the enzymatic hydrolysis of urea) in the solution at λ_{max} 385 nm, was measured to inspect the kinetics of the urease enzyme.

3. Results and discussions

3.1. Characterisation of ZrO_2 nanoparticles

The X-ray diffraction pattern of synthesised ZrO_2 nanoparticles reveals reflection planes that are consistent with ZrO_2 (Fig. 1(A). An average particle size of 12 nm was calculated from Debye-Scherer's formula [22] (Eq. (1)). The nanoparticle size deduced form Debye-Scherer's formula was also supported by the TEM analysis (Fig. 1(B)). The TEM image reveals predominantly spherical crystalline ZrO_2 nanoparticles with sizes varying from 8 nm to 25 nm (average size of ca 12 nm).

$$D = \frac{K\lambda}{BCos(\theta)} \quad (1)$$

Preparation of the ZrO_2-PPI dendrimer modified screen printed carbon electrode and the covalent immobilisation of the Urease enzyme

PPI dendrimers consist of peripheral 1° amine and internal 3° amines. The mechanism of the electrodeposition is based on the formation of an amine cation radical which creates a C—N linkage between the 1° amine of the dendrimer and the carbon electrode [23,24].

During the anodic scan, the 1° amines of the PPI dendrimers were electro-oxidised onto the bare SPCE surface to form a C—N bond between the SPCE and PPI. The scan shows the onset of the electro-oxidation and the generation of the free radical (Fig. 2). The bulk of the electro-deposition took place with the formation

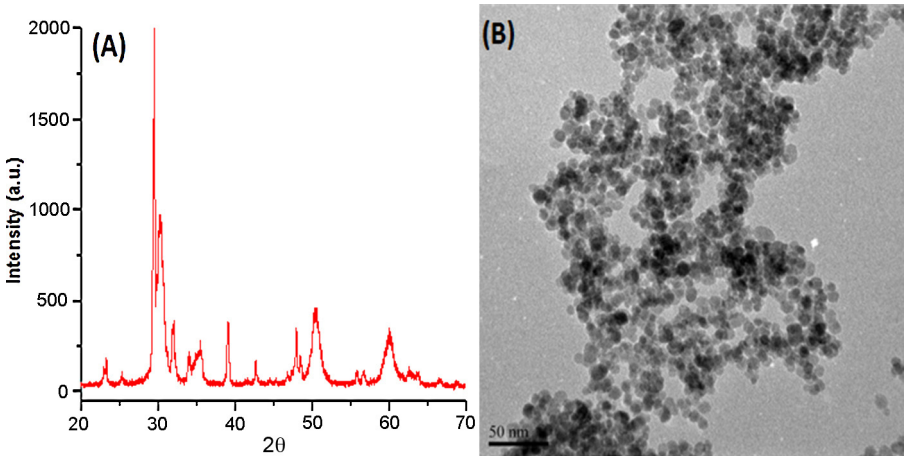

Fig. 1. X-ray diffraction pattern (A) and transmission electron micrograph (B) of ZrO_2 nanoparticle.

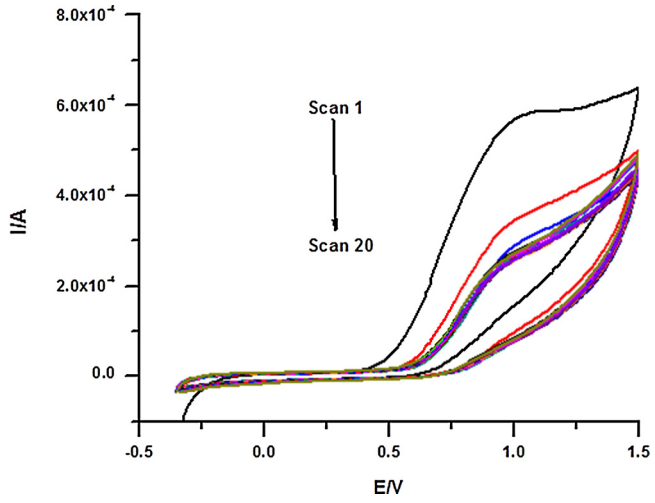

Fig. 2. Cyclic voltammograms of the co-electrodeposition of PPI/ZrO_2 nanocomposites from -0.3 V to 1.5 V for 20 cycles at scan rates of 50 mV s^{-1}.

of more oxidation radicals during the first scan while the subsequent scans were used to cover any available site on the SPCE – the reason for the reduced current peaks as number of scans increases.

Under the same condition of dendrimer deposition, ZrO_2 nanoparticles were simultaneously co-deposited with the PPI onto the SPCE. It is possible that surface charges of ZrO_2 nanoparticle interact with the cationic dendrimer matrix via electrostatic interactions and hydrogen bonding with $-NH_2$ groups to form hybrid nanocomposites [25]. This electro-co-deposition was substantiated by scanning electron microscopy (Fig. 3). The evidence of dendrimer electrodeposition can be seen by the homogenous nano-globular PPI on Fig. 3B in contrast to the bare SPCE (Fig. 3A). Fig. 3C shows that ZrO_2 nanoparticles were uniformly imbedded in the nano-globular PPI matrix and are stable with minimum aggregation. Furthermore, the energy dispersive X-ray spectroscopy (EDX) spectra (Fig. 3E) confirm the presence of Zr-atom in the ZrO_2-PPI nanocomposite electrode.

Urease is a family of phosphotriesterase and amidohydrolases and it catalyzes the hydrolysis of urea into ammonia and carbon dioxide. It composed of 3:3 (α:β) stoichiometric ratio with two folded symmetric structures with multi-active sites [26,27]. Urease molecules exist in anionic forms at pH 7.0. This anionic charge

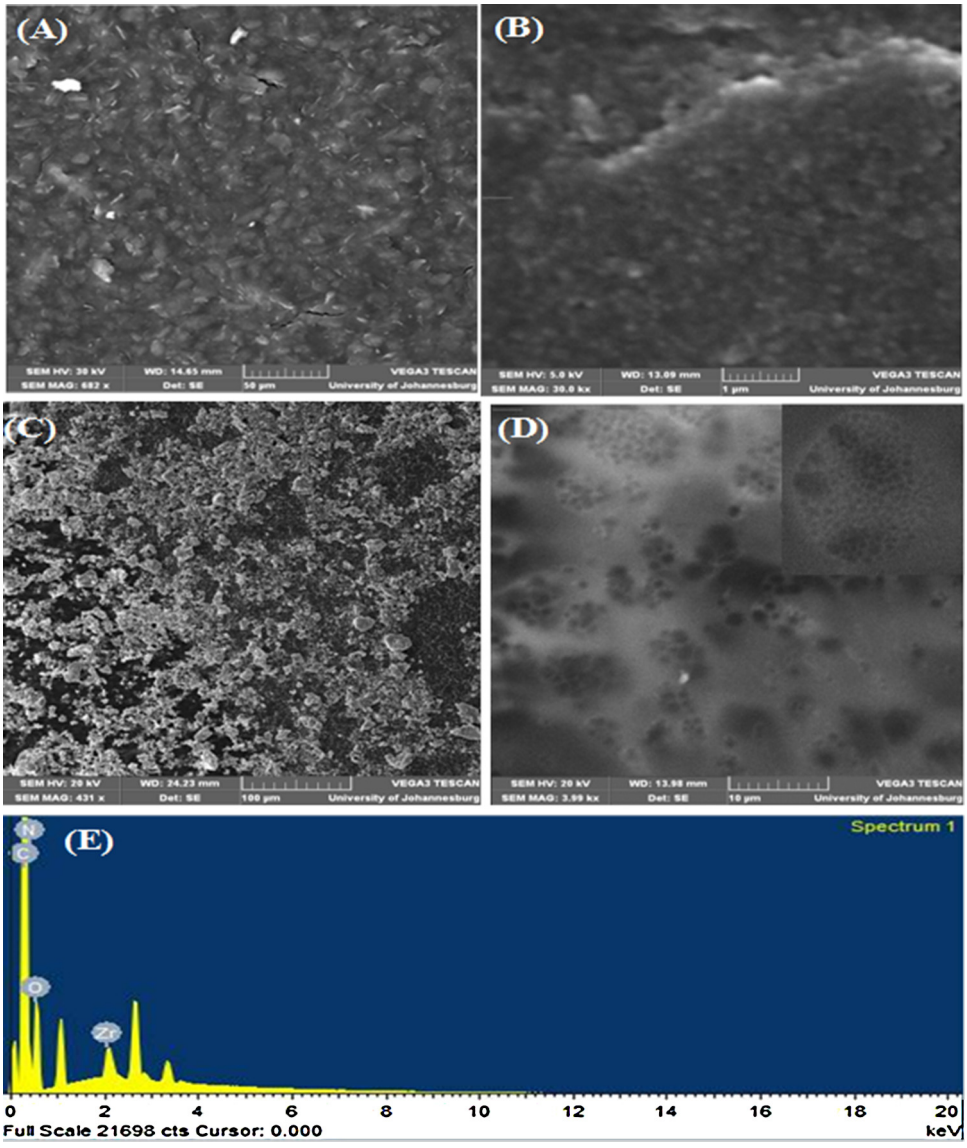

Fig. 3. SEM image of (A) bare, (B) PPI dendrimer, (C) ZrO_2-PPI dendrimer, (D) Urease/ZrO_2-PPI modified SPCE and (E) EDX spectra of ZrO_2-PPI dendrimer modified SPCE.

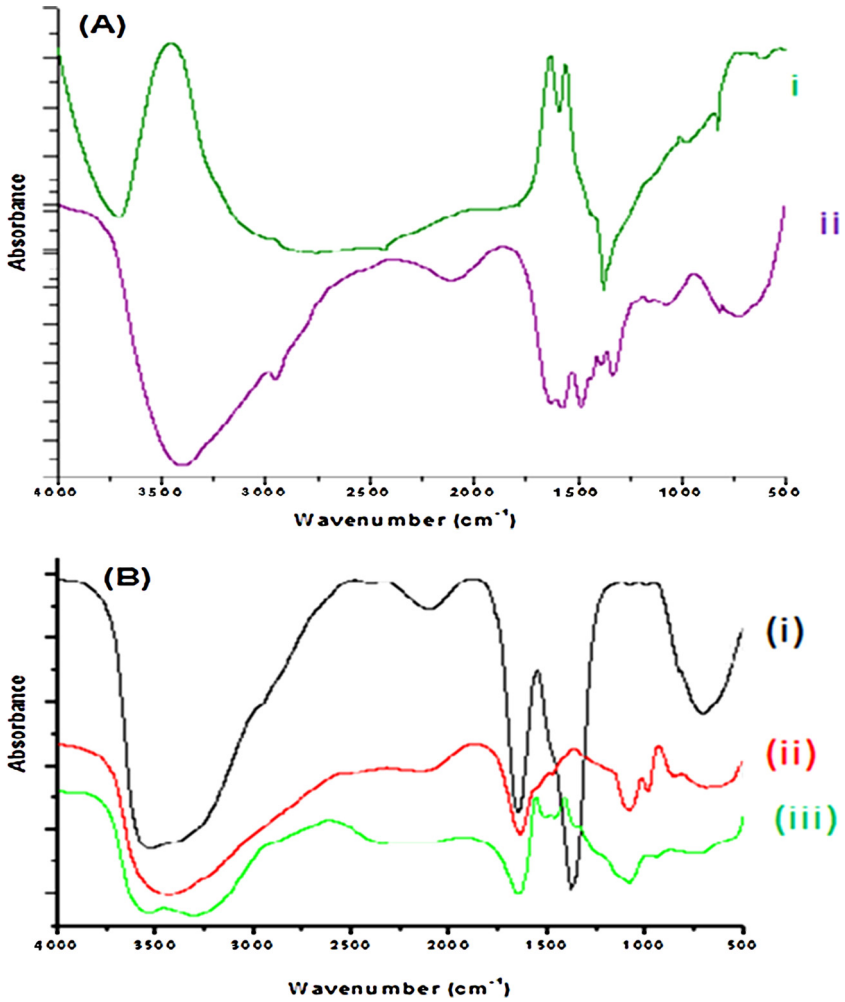

Fig. 4. FTIR spectra in KBr monitored in the region between 4000 cm^{-1} and 500 cm^{-1} (A) PPI dendrimer (i) and ZrO_2 nanoparticles (ii), (B) ZrO_2-PPI dendrimer (i), Urease/ZrO_2-PPI dendrimer (ii), Urease (iii).

can facilitate interaction with the positively charged PPI dendrimer via electrostatic interactions. The presence of ZrO_2 nanoparticles in the PPI matrix resulted in an increased electroactive surface area of PPI dendrimer which further improved the loading of enzymes onto the modified electrode. The immobilisation of urease was also confirmed with electrochemical and optical studies. The urease enzyme was immobilised onto the ZrO_2-PPI nanocomposite electrode via coupling chemistry using glutaraldehyde as a crosslinker. One end of the glutaraldehyde was attached to the ZrO_2/PPI/SPCE through a reaction between the terminal —NH_2 group of PPI and —CHO group of glutaraldehyde. The other end of —CHO group of glutaraldehyde was attached to the terminal —NH_2 group of urease, and this resulted in the formation of Urease/ZrO_2-PPI/SPCE urea active bioelectrode or urea biosensor. The immobilisation of the urease enzyme was supported by the obvious change in the morphology of the ZrO_2-PPI/SPCE after the immobilisation of the enzyme (Fig. 3D) [15,20,21,28].

The resultant enzyme immobilised electrode was characterised by FTIR spectroscopy (Fig. 4). FTIR spectra of ZrO_2 nanoparticles exhibited characteristic infrared absorption peak (curve (ii), Fig. 4A) at 622 cm^{-1} due to the symmetrical stretching of Zr—O—Zr species indicating the formation of zirconia nanoparticles. FTIR spectra of pure PPI dendrimer (curve (i), Fig. 4A) displayed bands at 3100 cm^{-1}–3600 cm^{-1} due to N—H stretching vibration; peak at 1574 cm^{-1} is attributed to the N—H deformation mode of —NH_2 group, while peak at 1490 cm^{-1} is attributed for to the symmetrical deformation of CH_2 group. In Fig. 4B(i), the N—H stretching mode of the dendrimer was also observed but at a lower wave number. This suggests that the —NH_2 group of PPI has interaction with the ZrO_2 nanoparticles in the formation of the ZrO_2-PPI nanocomposites. The FTIR spectrum of pure urease (Fig. 4B(iii)) exhibited several peak characteristic NH_2 groups and —COOH groups similar to that seen in the immobilised enzyme (Fig. 4B(ii)). The presence of 1646 cm^{-1} peak in Fig. 4B(ii) corresponding to amide bands confirms the formation of a peptide linkage between the urease and PPI via carbodiimide chemistry. The broadening in the range of 545 cm^{-1}–772 cm^{-1} with the shifting in the wavelength for zirconia, might be intermolecular interaction with enzymes. Hence, the FTIR spectra depicted the immobilisation of Urease onto ZrO_2-PPI nanocomposites matrix [5,29–33].

3.2. Electrochemical Studies of the modified electrodes

As depicted in Fig. 5, PPI/SPCE allowed for the reversible electrochemistry of $Fe(CN)_6]^{3-/4-}$. The $Fe(CN)_6]^{3-/4-}$ was markedly increased after dendrimer modification when compared to bare SPCE (not shown). The voltammograms in Fig. 5(a) show that PPI enhanced the interfacial electron transfer on the SPCE. The co-deposition of ZrO_2 nanoparticle further enhanced the redox peak (Fig. 5(b)) by improving the electroactive surface area and electrode conductivity. An expected reduction in redox peak (Fig. 5(c)) occurred after the immobilisation of the enzyme owing to its bulky

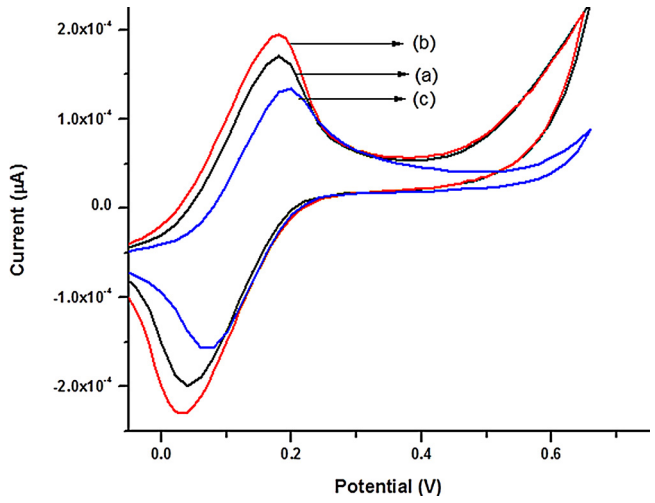

Fig. 5. Cyclic voltammetry studied of (a) PPI dendrimer, (b) ZrO_2-PPI dendrimer and (c) Urease/ZrO_2-PPI dendrimer modified SPCE. Recorded in PBS (50 mM, pH 7.0, 0.9% NaCl) containing 5 mM $[Fe(CN)_6]^{3-/4-}$ in the potential sweep of −0.1 V to +0.65 V at a scan rate of 50 mV s^{-1}.

molecular structure which hampers electron transfer. It should be noted however that presence of PPI and ZrO_2 nanoparticle wired the enzyme onto the electrode thereby facilitating electron transfer. This is one importance of using nanomaterial in biomolecular immobilisation–the conductive nanoparticle penetrates into the redox moiety located in the core of the enzyme facilitating electron shuttling between the enzyme and the electrode surface.

The surface concentration of the biosensor can be measured by using the Brown-Anson model [34]:

$$I_p = \frac{n^2F^2I^*AV}{4rt}$$

Where, n is the number of electrons transferred (i.e. 1), F is the Faraday constant (96,485 C/mol), I^* is the surface concentration of respective electrodes, A is the surface area of the electrode (0.14 cm^2), V is the scan rate (50×10^{-3} V s^{-1}), R is the gas constant (8.314 J mol^{-1} K^{-1}) and T is the room temperature (298 K). The surface concentration of ZrO_2-PPI/SPCE (2.965×10^{-8} mol cm^{-2}) than that of PPI/SPCE (1.0159×10^{-8} mol cm^{-2}).The higher concentration of ZrO_2-PPI electrode suggests that loading of the ZrO_2 nanoparticles augments the electroactive surface area.

Cyclic voltammetric studies were carried out with Urease/ZrO_2-PPI/SPCE bioelectrodes in PBS (50 mM, 0.9% NaCl and pH 7.0) containing 5 mM $[Fe(CN)_6]^{3-/4-}$ as a function of scan rates varying from 10 mV s^{-1} to 200 mV s^{-1} (Supplementary 1A). It can be found that both the cathodic (I_c) as well as anodic (I_a) peak currents of the electrode increase linearly and are proportional to the scan rate (Supplementary 1B).

The values of heterogeneous electron rate transfer constant (ks) have been calculated using Laviron's model [35,36] for Urease immobilised ZrO_2-PPI dendrimer nanocomposite/SPCE:

$$k_s = \frac{mnF\upsilon}{RT}$$

Where ks is the electron rate transfer constant, m is peak to peak separation, n is number of electrons transferred (1), F is Faraday constant (96485 J), υ is scan rate (50 mV s^{-1}), R is gas constant (8.314 J K^{-1} mol^{-1}) and T is absolute room temperature (298 K). The value of electron rate transfer constant (ks) obtained (2.02 s^{-1}), is higher than that of earlier reported nanoparticle based biosensors [30,37–40].

3.3. Urea biosensing and interference studies

The prepared Urease/ZrO_2-PPI nanocomposite modified SPCE was applied for the amperometric detection of urea at a constant potential of 0.8 V (the oxidation of ammonia to nitrogen occurs at this potential) [41]. A steady increase in current with increasing concentration of urea was observed (Fig. 6A (zones A and C). The effect of potential interferents (ascorbic acid, uric acid, glucose, and lactate) on the Urease/ZrO_2-PPI/SPCE was explored. The interferents were added at their normal physiological concentrations, i.e. ascorbic acid (2 mM), lactate (2 mM); glucose (5 mM) and uric acid (0.2 mM). Negligible effects were observed for all the interferents as depicted in the marked interference zone B in Fig. 6A, where very minimal current increases were observed upon the addition of the interferents. From zone C, it was observed that the biosensor responded sharply again to urea even in the presence of the already present interferents.

A calibration plot of the biosensor response to urea in Fig. 6A is plotted as Fig. 6B. The amperometric response increased linearly in the range of 0.01 mM to 2.99 mM. The linear regression equation is I (μA) = 3.89x + 0.42 with correlation coefficient (R^2) of 0.9985. The current sensitivity in the linear range of the proposed urease biosensor towards urea concentration was 3.89 μA mM^{-1} cm^{-2}.

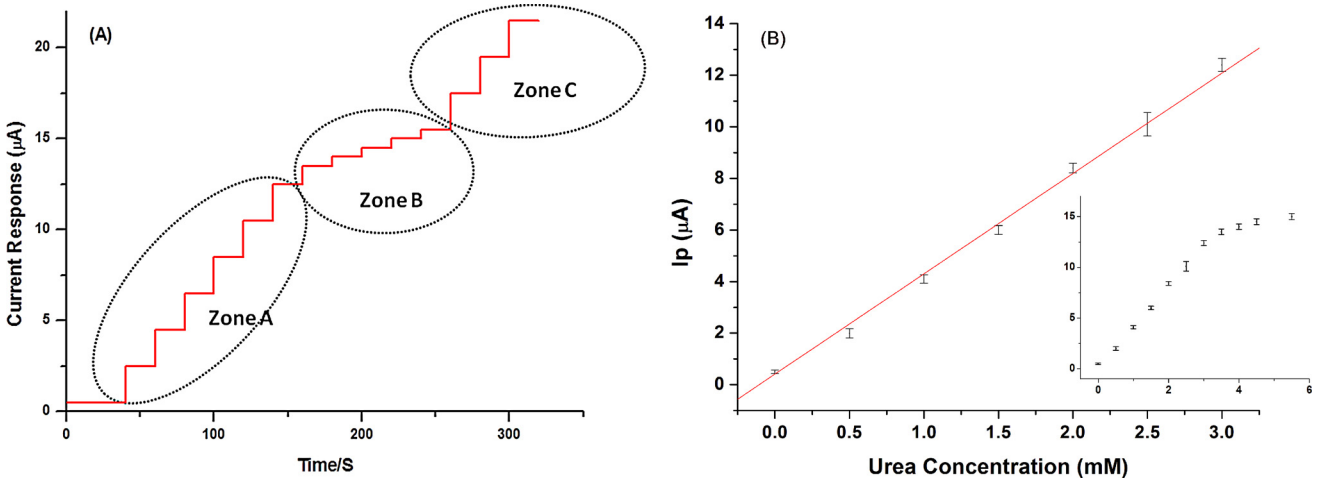

Fig. 6. (A) Amperometric response of urease/ZrO_2-PPI dendrimer/SPC bioelectrode on successive addition of 1.5 mM urea to a 0.1 phosphate buffer solution (pH 7.5) solution. Potential poised at +800 mV; solution stirring at 200 rpm (A) Where zone A = addition of urea, Zone B addition of inteferents and Zone C addition of urea. (B) Corresponding calibration plot between current vs urea concentration (B).

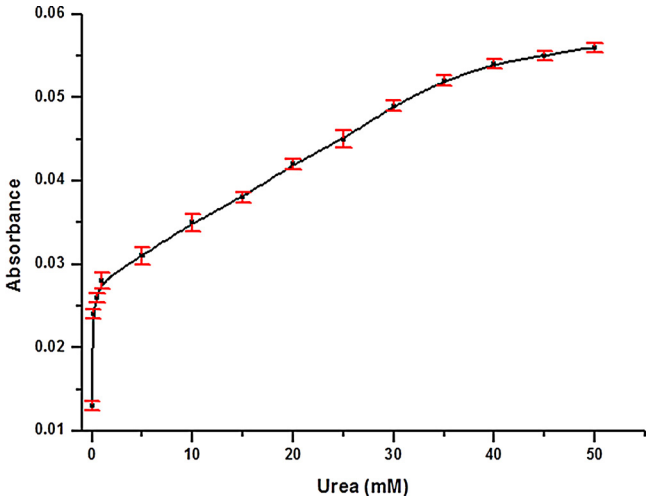

Fig. 7. Photometric response of ZrO_2-PPI/SPCE as a function of urea concentration.

3.4. Photometric response studies

Photometric studies were carried out to calculate the apparent enzyme assay activity, stability and shelf life of the urease/ZrO_2-PPI/SPCE based urease biosensor. The fabricated bioelectrode was dipped for 3 min into 3.0 ml of PBS solution (pH 7.5) containing 15 μl of Nessler's reagent solution and 100 μl of urea in varying concentrations (0.01 mM to 50 mM). The immobilised urease enzyme on the surface of ZrO_2-PPI dendrimer nanocomposite modified SPCE matrix catalyzed the hydrolysis of urea and produced ammonia, which reacted with Nessler's reagent ($K_2Hg_2I_4$) to form a coloured product (i.e. $NH_2Hg_2I_3$) (Supplementary 2) resulting in changes in absorbance [3,42]. The differences between the final and initial absorbance of the biosensor at a fixed wavelength ($\lambda = 385$ nm), was measured and corresponding values plotted against as a function of urea concentration (Fig. 7).

The noticeable apparent enzyme activity of the urease functionalized ZrO_2-PPI dendrimer based urea biosensor was calculated using the equation;

$$\alpha_{app}^{enz} = \frac{AV}{\epsilon_{st}}$$

Where, A is the difference in the absorbance before and after incubation of the biosensor in the saturated solution, V is the total volume (3.0 cm^3), ε is the millimolar extinction coefficient of Nessler's reagent, t is the reaction time (3 min) and s is the surface area of the bioelectrode. The calculated value of apparent enzyme activity was found to be ca 76.38 mg cm^{-2}, indicating that 76.38 mg of urease enzyme per cm^2 actively participated in the enzymatic reaction per unit area of biosensor.

4. Conclusion

This work describes the preparation of a novel dendrimer–zirconia nanocomposite as suitable nano-platform for enzyme immobilisation. The biocompatibility and host guest capability of poly(propylene imine) dendrimer towards biomaterial such as urease enzyme are demonstrated by the plausible biosensor response to urea in about 4 s. The fact that the urease enzyme retained its activity (as depicted by the photometric studies) showed the biocompatibility of both zirconia and the dendrimer. The electrode preparation and enzyme immobilisation steps are simple and straight forward. The chemical tunability of poly(propylene imine) dendrimer and dendrimer in general, affords the preparation of a wide range of as nanocomposite platforms which can explored in the development of biosensors.

Acknowledgements

The financial support of the following is gratefully acknowledged: The Centre for Nanomaterial Science Research, Department of Applied Chemistry, University of Johannesburg; and the Faculty of Science, University of Johannesburg. The authors also wish to thank Mr. Patrick Mubiayi, Extraction Metallurgy Laboratory, University of Johannesburg for carrying out the SEM characterisation.

Appendix A. Supplementary data

Supplementary data associated with this article can be found, in the online version, at http://dx.doi.org/10.1016/j.enzmictec.2014.08.003.

References

[1] Ivanova S, Ivanov Y, Godjevargova T. Urea amperometric biosensors based on nanostructured polypyrrole and poly ortho-phenylenediamine. Open J Appl Biosens 2013;2:12–9.
[2] Guyton AC. Blood pressure control-special role of the kidney and body fluids. Science 1991;252:1813–6.
[3] Tiwari A, Aryal S, Pilla S, Gong S. An amperometric urea biosensor based on covalently immobilized urease on an electrode made of hyperbranched polyester functionalized gold nanoparticles. Talanta 2009;78:1401–7.
[4] Dhawan G, Sumana G, Malhotra BD. Recent developments in urea biosensors. Biochem Eng J 2009;44:42–52.
[5] Sumana G, Das M, Srivastava S, Malhotra BD. A novel urea biosensor based on zirconia. Thin Solid Films 2010;519:1187–91.
[6] Singh M, Verma N, Garg AK, Redhu N. Urea biosensors. Sens Actuators B 2008;134:345–51.
[7] Pandey P, Datta M, Malhotra BD. Prospects of nanomaterials in biosensor. Anal Lett 2008;41:157–67.
[8] Kaushik A, Khan R, Solanki PR, Pandey P, Alam J, Ahmad S, Malhotra BD. Iron oxide nanoparticles-chitosan composite based glucose biosensor. Biosens Bioelectron 2008;24:676–83.
[9] Wang SF, Tan YM. A novel amperometric immunosensor based on Fe_3O_4 magnetic nanoparticles/chitosan composite film for determination of ferritin. Anal Bioanal Chem 2007;387:703–8.
[10] Pandey P, Singh SP, Arya SK, Gupta V, Datta M, Singh S, Malhotra BD. Application of thiolated gold nanoparticles for enhancement of glucose oxidase activity. Langmuir 2007;23:3333–7.
[11] Yang Y, Yang H, Yang M, Liu Y, Shen G, Yu R. Amperometric glucose biosensor based on a surface treated nanoporous ZrO_2/chitosan composite films as immobilization matrix. Anal Chim Acta 2004;525:213–20.
[12] Liu S-Q, Xu J-J, Chen H-Y. ZrO_2 gel-derived DNA-modified electrode and the effect of lanthanide on its electron transfer behavior. Bioelectrochemistry 2002;57:149–54.
[13] Arotiba OA, Ignaszak A, Malgas R, Al-Ahmed A, Baker PGL, Mapolie SF, Iwuoha EI. An electrochemical DNA biosensor developed on novel multinuclear nickel(II) salicylaldimine metallodendrimer platform. Electrochim Acta 2007;53(4):1689–96.
[14] Arotiba OA, Baker PG, Mamba BB, Iwuoha EI. The application of electrodeposited poly(propylene imine) dendrimer as an immobilization layers in a simple electrochemical DNA biosensor. Int J Electrochem Sci 2011;6:673–83.
[15] Shukla SK, Mishra AK, Mamba BB, Arotiba OA. Amperometric and photometric of in situ coupled glucose oxidase-poly(propylene imine) dendrimer based glucose biosensor. Int J Electrochem Sci 2013;8:11711–22.
[16] Tomalia DA, Naylor AM, Goddard III WA. Starburst dendrimers: molecular-level control of size, shape, surface chemistry, topology, and flexibility from atoms to macroscopic matters. Angew Chem 1990;29:138–75.
[17] Frechet JM. Functional polymers and dendrimers: reactivity, molecular architecture, and interfacial energy. Science 1994;263:1710–5.
[18] Kavosi B, Salimi A, Hallaj R, Amani K. A highly sensitive prostate-specific antigen immunosensor based on gold nanoparticles/PAMAM dendrimer loaded MWCNTS/chitosan/ionic liquid nanocomposite. Biosens Bioelectron 2013;52:20–8.
[19] Aranishi K, Singh AK, Xu Q. Dendrimer-encapsulated bimetallic Pt-Ni nanoparticles as highly efficient catalysts for hydrogen generation form chemical hydrogen storage materials. Chem Cat Chem 2013;5(8):2248–52.
[20] Arotiba OA, Owino J, Songa E, Hendricks N, Waryo T, Jahed N, Baker PG, Iwuoha EI. An electrochemical DNA biosensor developed on a nanocomposite platform of gold and poly(propyleneimine) dendrimer. Sensors 2008;8(11):6791–809.
[21] Arotiba OA, Songa EA, Baker PG, Iwuoha EI. Dendrimeric gold-poly (propylene imine) electrochemical DNA nanobiosensor. Chim Oggi 2009;27:55–8.
[22] Shukla SK, Agorku ES, Mittal H, Mishra AK. Synthesis: characterization and photoluminescence properties of Ce3 + -doped ZnO-nanophosphors. Chem Pap 2014;68(2):217–22.

[23] Deinhammer RS, Ho M, Anderegg JW, Porter MD. Electrochemical oxidation of amine-coating compounds: A route to the surface modification of glassy carbon electrodes. Langmuir 1994;10:1306–13.
[24] Downard AJ. Electrochemically assisted covalent modification of carbon electrodes. Electroanalysis 2000;12:1085–96.
[25] Yang Y, Yang H, Yang M, Liu Y, Shen G, Yu R. Amperometric biosensor based on a surface treated nanoporous ZrO_2/chitosan composite film as immobilization matrix. Anal Chim Acta 2004;525:213–20.
[26] Kuralay F, Ozyoruk H, Yildiz A. Amperometric enzyme electrode for urea determination using immobilized urease in poly(vinylferrocenium) films. Sens Actuators B 2006;114:500–6.
[27] Holm L, Sander C. An evolutionary treasure: unification of a broad set of amidohydrolases related to urease. Protein 1997;28:72–82.
[28] Chen J-P, Chiu S-H. A poly(*N*-isopropylacrylamide-*co*-*N*-acryloxysuccinimide-*co*-2-hydroxyethyl methacrylate) composite hydrogel membrane for urease immobilization to enhance urea hydrolysis rate by temperature swing. Enzyme Microb Technol 2000;26:359–67.
[29] Shukla SK, Deshpande SR, Shukla SK, Tiwari A. Fabrication of a tunable glucose biosensor based on zinc oxide/chitosan-*graft*-poly (vinyl alcohol) core-shell nanocomposites. Talanta 2012;99:283–7.
[30] Kaushik A, Solanki PR, Ansari AA, Sumana G, Ahmad S, Malhotra BD. Iron oxide-chitosan nanocomposites for urea sensor. Sens Actuators B 2009;138:572–80.
[31] Salimi A, Noorbakhsh A. Layer by layer assembly of glucose oxidase and thiourea onto glassy carbon electrode: fabrication of glucose biosensor. Electrochim Acta 2011;56(17):6097–105.
[32] Solanki PR, Kaushik A, Ansari AA, Tiwari A, Malhotra BD. Multi-walled carbon nanotubes/sol-gel derived silica/chitosan nanobiocomposite for total cholesterol sensor. Sens Actuators B 2009;137:727–35.
[33] Reddy MM, Reddy DJ, Moin A, Shivakumar HG. Formulation of sustained matrix tablet using chitosan/ghatti gum polyelectrolyte complex. Der Pharmacia Lettre 2011;3(2):119–28.
[34] Singh J, Kalita P, Singh MK, Malhotra BD. Nanostructured Nickel oxide-chitosan film for application to cholesterol sensor. Appl Phys Lett 2011;98:123702–3.
[35] Laviron E. General expression of the linear potential sweep voltammograms in case of diffusionless electrochemical systems. J Electroanal Chem 1979;101:19–28.
[36] Aleveque O, Blanchard PY, Gautier C, Dias M, Breton T, Levillain E. Electroactive self-assembled monolayers: Laviron's interaction model extended to non-random distribution of redox centers. Electrochem Commun 2010;12(11):1462–6.
[37] Chen X, Ruan C, Kong J, Deng J. Characterization of the direct electron transfer and bioelectrocatalysis of horseradish peroxidase in DNA film at pyrolytic graphite electrode. Anal Chim Acta 2000;412:89–98.
[38] Topoglidis E, Astuti Y, Duriaux F, Gratzel M, Durrant JR. Direct electrochemistry and nitric oxide interaction of heme proteins adsorbed on nanocrystalline tin oxide electrodes. Langmuir 2003;19:6894–900.
[39] Zhao YD, Bi YH, Zhang WD, Luo QM. The interface behavior of haemoglobin at carbon nanotube and the detection for H_2O_2. Talanta 2005;65:489–94.
[40] Zhang L, Jiang X, Wang E, Dong S. Attachment of gold nanoparticles to glassy carbon electrode and its application for the direct electrochemistry and electrocatalytic behavior of haemoglobin. Biosens Bioelectron 2005;21:337–45.
[41] Gabrovska K, Ivanov J, Vasileva I, Dimova N, Godjevargova T. Immobilization of urease on nanostructured polymer membrane and preparation of urea amperometric biosensor. Int J Biol Macromol 2011;48:620–6.
[42] Bisht RVW, Takashima K. A novel thin film urea biosensor based on copolymer poly(*N*-3aminoprpyrrole-*co*-pyrrole) film. Surf Coat Technol 2005;198(1-3):231–6.